DIRECT NUMERICAL SIMULATION OF TURBULENT REACTING JET INTRODUCING FULLY DEVELOPED TURBULENCE AT THE INLET

Shuichiro Hirai, Masanori Takeno and Kiyotaka Hiradate

Research Center for Carbon Recycling and Energy,
Tokyo Institute of Technology,
2-12-1, Ohokayama, Tokyo, 152-8552, Japan
hirai@mes.titech.ac.jp

ABSTRACT

Fully developed turbulent reacting jet formed by introducing inlet condition given by a turbulent channel flow was analyzed by the data base of direct numerical simulation. We show characteristic reacting processes that product concentration increases rapidly at the region further than a distance similar to that of channel width from the jet inlet. Detailed interpretation has been made to elucidate the interactions between vortices and mixing/reaction processes . Rapid increase is mainly caused by an increase of reaction zone thickness, not its length. Cloud-like reaction zones are formed, which are related to vortices expanding toward outer regions accompanied by change of vortex structure. Counter-rotating vortices are observed in some cloud-like reaction zones where reactants intrude each other.

INTRODUCTION

Turbulent reacting jet is of considerable importance for understanding flow, mixing and combustion processes and mechanisms in furnaces and combustors. Because the interactions between the reaction processes and the turbulence are complex, a direct numerical simulation (DNS) solving the time-dependent transport equations of momentum, concentrations and energy is an effectual method that could obtain fundamental understanding from the database of instantaneous three dimensional physical properties, i.e., velocities, temperature, concentrations, etc.

Many DNS studies have been performed focussing on non-premixed type combustion, which is encountered in many practical furnaces. An extended review was presented for direct numerical simulation of non-premixed turbulent flames (Vervish and Poinsot, 1998). The study by McMurtry et al. using DNS of time-developing reacting mixing layer focused on how heat release effect on the vorticity dynamics (McMurtry et al, 1989). It was elucidated that the amount of mass entrainment into the layer is reduced as the rate of heat release increases and heat release has a significant effect on the vortex characteristics. The interactions between hydrogen-air diffusion flames and large-scale structures in the mixing layer are investigated by conducting direct numerical simulation of two-dimensional temporally developing chemically reacting mixing layer (Li et al, 1999). These studies were performed on time-developing mixing layer (McMurtry et al, 1989, Li et al, 1999). Other DNS studies used decaying isotropic turbulence, which are those of three dimensional DNS of turbulent non-premixed flames including finite-rate chemistry and heat release effects (Mahalingam et al, 1995) and autoignition of nonpremixed turbulent flame (Hilbert et al, 2002).

Spatially fully developed turbulent jet has some difficulty in performing DNS. Inlet streams given in laminar flows need long distance to develop into turbulence, which was shown by a classical experimental study of mixing layer where two gas streams of different velocities form Kelvin-Helmholtz type vortices that show mixing transition at the far downstream region to be a developed turbulence (Brown and Roshko, 1974). Without mixing transition, Sotriou and Ghoniem (1995) studied the applicability of an infinite reaction model in the simulations of an exothermic mixing layer. With mixing transition, direct numerical simulation of a non-reacting three-dimensional spatially developing turbulent mixing layer was investigated to make clear the structures of the mixing layer and the budgets of the transport equations of Reynolds stresses (Miyauchi et al., 1996).

Direct numerical simulation of turbulent reacting jet we conducted introduced fully developed turbulence at the jet inlet. The turbulent jet needs a relatively small calculation region in streamwise direction, which is suitable for DNS. This configuration was determined taking account not only for DNS but for practical sense of furnaces and combustors.

Especially, in many non-premixed type ones, fuel is introduced through a nozzle in which turbulent vortices are formed. Fuel in vortical motion is released to the open space where it is mixed with surrounding air flow. Fuel and air react with each other at the reaction zone affected by the vortices, developed inside the nozzle, altering their shape at the mixing region. Thus, the configuration of the present DNS study is often encountered in practical furnaces and combustors.

We show that, in DNS of the turbulent jet, product con-

centration shows a characteristic profile which is affected by mixing and reaction due to the vortices introduced to the inlet. Detailed interpretation for the interactions between vortices and mixing/reaction processes has been presented.

NOMENCLATURE

Ce	Ce number
Da	Damkohler number
F	reactant (fuel)
L	interfacial length of reaction zone
M	Mach number
O	reactant (oxidizer)
P	product
p	nondimensional pressure
ρ	non-dimensional density
Pr	Prandtle number
Q	second invariant of velocity gradient tensor
Re	Reynolds number
Sc	Shmidt number
T	non-dimensional temperature
t	non-dimensional time
$\mathbf{u}$	velocity vector
u	velocity in x direction
u_m	streamwize velocity at the outlet averaged over z direction
v	velocity in y direction
w	velocity in z direction
x	coordinate in streamwize direction
y	coordinate normal to the wall direction
Y_i	mass fraction of chemical species i
$[Y_p]_{y-z}$	integration of Y_p over a y-z plane
$[Y_F Y_O]_{y-z}$	integration of $Y_F Y_O$ over y-z plane
z	coordinate in spanwize direction

GREEK SYMBOLS

Δr	thickness of reaction zone
γ	ratio of heat capacity
τ	viscous stress tensor

BASIC EQUATIONS AND CALCULATION PROCEDURE

The calculation is based on three-dimensional time-dependent compressible conservation equations of mass, momentum, energy, chemical species and equation of state. They are written in non-dimensional forms, scaled by the friction velocity, distance between channel walls, density and temperature of the jet inlet.

$$\frac{\partial \rho}{\partial t} + \nabla \cdot (\rho \mathbf{u}) = 0 \tag{1}$$

$$\frac{\partial \mathbf{u}}{\partial t} + (\mathbf{u} \cdot \nabla)\mathbf{u} = -\frac{1}{\rho}\frac{1}{\gamma M^2}\nabla p + \frac{1}{\rho}\frac{1}{\mathrm{Re}}\nabla \cdot \tau \tag{2}$$

$$\frac{\partial T}{\partial t} + (\mathbf{u} \cdot \nabla)T = \frac{1}{\rho}\frac{\gamma}{\mathrm{Pr} \cdot \mathrm{Re}}\nabla^2 T - (\gamma - 1)\frac{1}{\rho} p \nabla \cdot \mathbf{u} + \frac{\gamma(\gamma-1)M^2}{\mathrm{Re}}\frac{1}{\rho}\tau \cdot \nabla \mathbf{u} + Ce \cdot Da \rho Y_F Y_O \tag{3}$$

$$\frac{\partial Y_i}{\partial t} + (\mathbf{u} \cdot \nabla)Y_i = -\frac{1}{\rho \mathrm{Re} \cdot \mathrm{Sc}}\nabla \cdot (-\rho \nabla Y_i) - Da \rho Y_F Y_O \tag{4}$$

$i = F, O$

$$p = \rho T \tag{5}$$

Non dimensional parameters included in the above equations are settled as follows.

$Re = 300$, $Pr = 0.7$, $Sc = 1.3$, $M = 0.03$, $Da = 1.0$, $Ce = 2.0$

Schematic views and the geometry of the computational domain of turbulent channel flow and turbulent jet is depicted in Fig. 1. Fully developed wall turbulence, using cyclic condition in streamwise direction, was formed using a channel flow, has a computational domain, of 3.8 for direction x, 1.0 for y and 1.92 for z. 32 and 128 grids are used in streamwise x and spanwize z directions, respectively, and 64 grid points with nonuniform spacing was distributed in the y (normal to the wall) direction. Grid points are concentrated near the wall so as to resolve the viscous sublayers. Instantaneous velocity in y-z plane was cut and introduced to the jet inlet. The size of the computational domain is 4.11 for the mean flow direction x, 4.16 for the transverse to the mean flow direction y and 1.92 for spanwize direction z. The spacing in y direction used in channel flow was continuously used in the turbulent jet calculation region. (region 1.00 depicted in Fig.1). At the outer surrounding flow region (region 1.58 in Fig. 1), the grid spacing inside (turbulent jet side) was turned round so as to serve sufficient resolving at the mixing region. Spacing and grid points in z direction are the same of that in channel. In x direction, grid spacing are concentrated at the inlet to resolve drastic change of vertices released in the open space. To let vortices smoothly flow out the calculation region without unexpected disturbance, calculation region with length of 10.75 in streamwise direction was settled at the outlet region, where Reynolds number was gradually decreased to diminish vortices so that fluid without vortices flow out the outlet plane. A condition at the outlet plane was settled using the following equation,

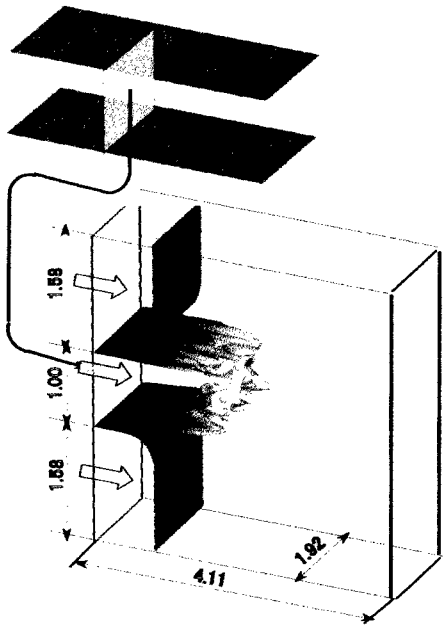

Fig. 1 Schematic view of spatially developing reacting jet

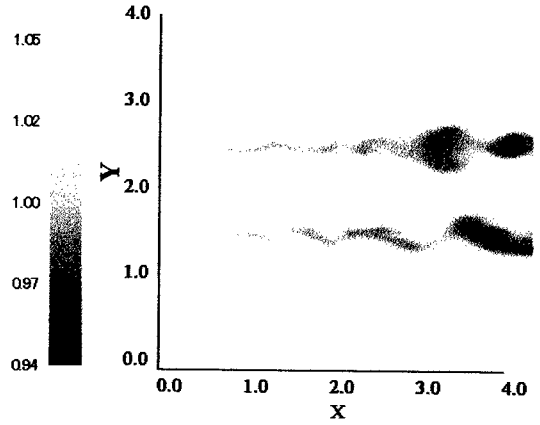

Fig. 2 Contour of instantaneous density in y-z plane

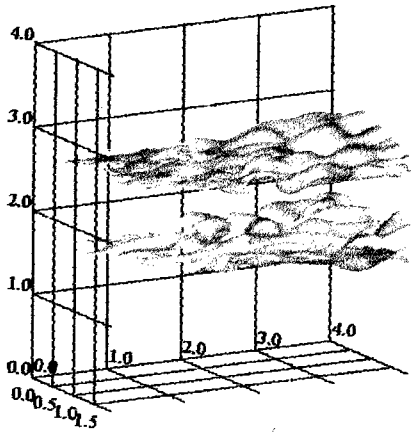

Fig. 3 Contour of instantaneous mass fraction of product Y_P

$$\frac{\partial u}{\partial t}+u_m\frac{\partial u}{\partial t}=\frac{1}{\rho}\frac{1}{\mathrm{Re}}\frac{\partial \tau_{ij}}{\partial x_j} \tag{6}$$

The surrounding flow velocity is 0.5 times as large as that of turbulent jet. No disturbance was added to the surrounding flows. The reactant F enters the computational domain on the central turbulent jet, while the other reactant O enters on both upper and lower surrounding flows. The chemical reaction applied here is a single-step, irreversible reaction,

$$F+O\rightarrow 2P. \tag{7}$$

Fifth order upwind scheme (Rai and Moin, 1991) was used for convection terms and 4th-order Runge-Kutta scheme for time integration.

RESULTS AND DISCUSSIONS

Prior to show the results, we stress that the target of the present study is to obtain a fundamental understanding on reaction processes of turbulent jet, not on combustion. Turbulent transport including reaction processes are dominated by various factors in which heat release is known to have an large effect on vortical structure (McMurty, 1989). Therefore, Da and Ce numbers are set to be small so as to set the effect of heat release, and further effect of density to be negligibly small (Figure 2).

Contour of instantaneous mass fraction of product Y_P is depicted in Figure 3. Fuel F on the turbulent jet reacts with O at two sides, upper and lower surrounding flows. At each region, thin contour at upstream region split into two layers, because contour of product P has a finite thickness at the down stream region and cyclic condition was employed in z direction. Thickness and surface undulation increase at the downstream.

In order to evaluate the characteristics variation of mass fraction of product Y_P quantitatively, we define $[Y_P]_{y\text{-}z}$,

$$[Y_P]_{y-z}=\iint_{y-z\_plane} Y_P dydz \tag{8}$$

Variation of $[Y_P]_{y\text{-}z}$ with the mean flow direction x, is depicted in Fig 4. $[Y_P]_{y\text{-}z}$ increases rapidly in the range x>1.0 compared with that in 0<x<1.0.

Because product P is produced by the production term, $Da\rho Y_F Y_O$ due to the reaction, change of $[Y_F Y_O]_{y\text{-}z}$, defined as

$$[Y_F Y_O]_{y-z}=\iint_{y-z\_plane} Y_F Y_O dydz \tag{9}$$

with x, is depicted in Fig. 5. $[Y_F Y_O]_{y\text{-}z}$ clearly shows a rapid increase at the region x>1.0, which corresponds to the tendency of $[Y_P]$ observed in Fig. 4.

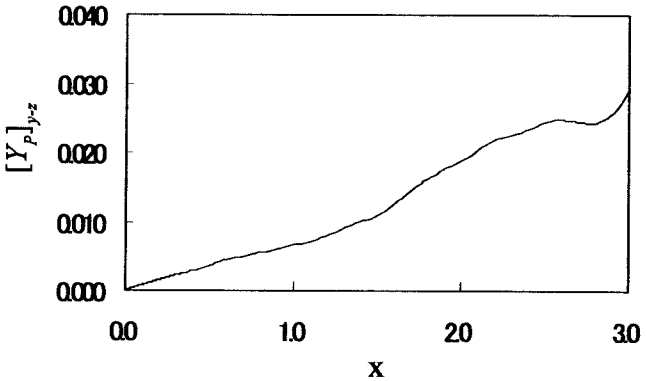

Fig. 4 Variation of $[Y_P]_{y\text{-}z}$ with x

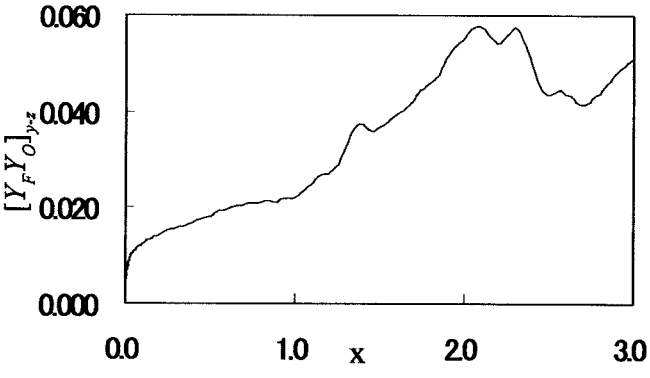

Fig. 5 Variation of $[Y_F Y_O]_{y\text{-}z}$ with x

profile, rapid increase in the range x>1.0, the instantaneous contours of $Y_F Y_O$ in y-z plane at x=0.5 (0<x<1.0) and x=2.0 (x>1.0) are shown in Figs. 6(a) and (b), respectively. Reaction take place where $Y_F Y_O$ is large and contour of $Y_F Y_O$ show large difference between upstream (x=0.5) and downstream (x=2.0) locations. Enhanced mutual intrusion and diffusion of reactants F and O leads to curved and thick $Y_F Y_O$ regions (Fig. 6(b), x=2.0). On the other hand, only small fluctuation at the interface is observed in x=0.5 (Fig.6(b)).

Further consideration has been made to elucidate the increase of reaction zone. We extracted reaction zone where $Y_F Y_O$ is larger that 0.2. The reaction zone is decomposed into two parameters, interfacial length L and mean thickness of reaction zone Δr, which are shown in Figs. 7 and 8, respectively. It can be clearly seen from these figures that rapid increase of $Y_F Y_O$ in the range x>1.0 is caused by increase of thickness of reaction zone Δr which shows the same tendency observed in Fig.5. Increase of interfacial length L in x=1.0 is only 20% larger than that in x=2.0, whereas Δr increases by a factor 2.

We again consider the instantaneous reaction zone depicted in Fig. 6. Thickness of the reaction zone in x=0.5 (Fig.6. (a)) is nearly constant and thin, whereas some thick cloud-like thick zone appears in x=2.0 (C, D in (Fig.7 (b)). Increase of reaction zone thickness in x=2.0 is not constant.

Instantaneous reaction zones of A, B (in Fig.6 (a))and C, D (in Fig.6 (b)) are depicted in Figs. 9 along with velocity vectors in y-z plane. Velocity vectors in A and B shows that vortices exist in a region inside the reaction zone (jet side), whereas those in C and D exist crossing it. Counter-rotating vortices drive mutual intrusion of reactants F and O into each other side to form "cloud-like" reaction zones.

The difference of these characteristic reaction zones between downstream and upstream are considered to be caused by the change of vortical nature. Turbulent vortices are visualized by second invariant of velocity gradient tensor Q in Fig. 10. Fig. 10 (a) is to show in three dimensional features and (b) from the side view point to see parallel to z (spanwize) axis. Positive region of Q shows solid body rotational region in vortices. Fig. 10 (a) shows that vortices, developed inside

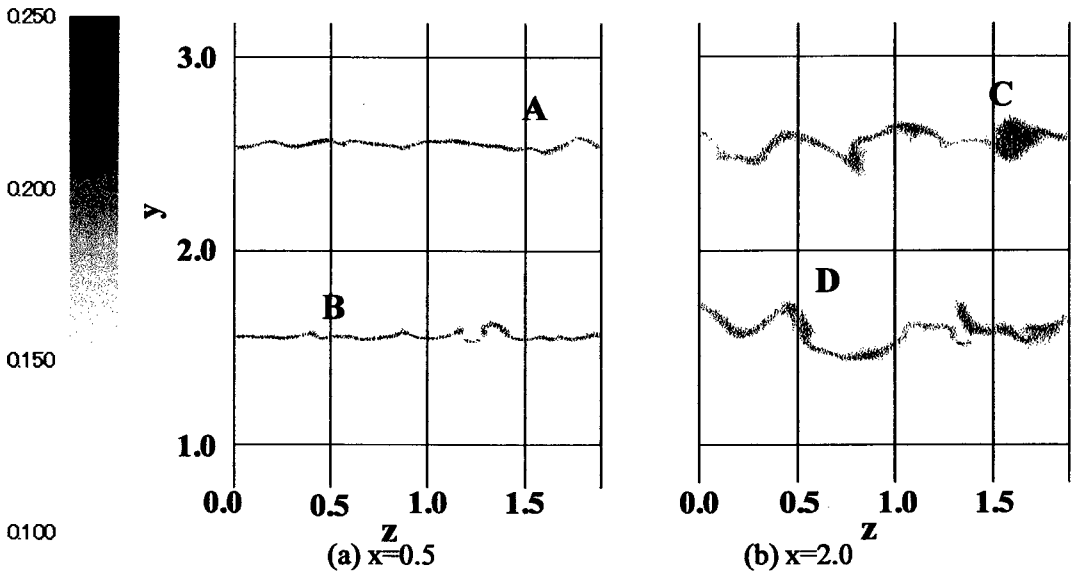

Fig. 6 Contours of $Y_F Y_O$ in y-z plane

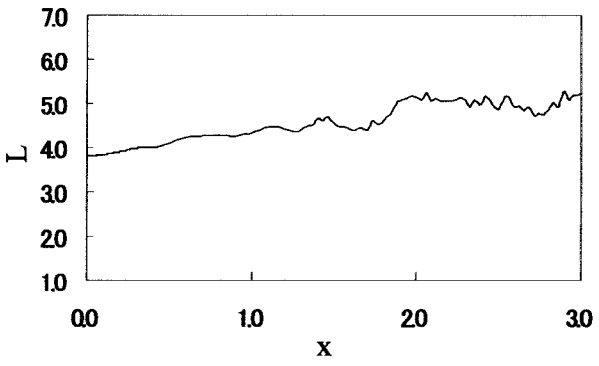

Fig. 7 Variation of interfacial length of reaction zone L with x

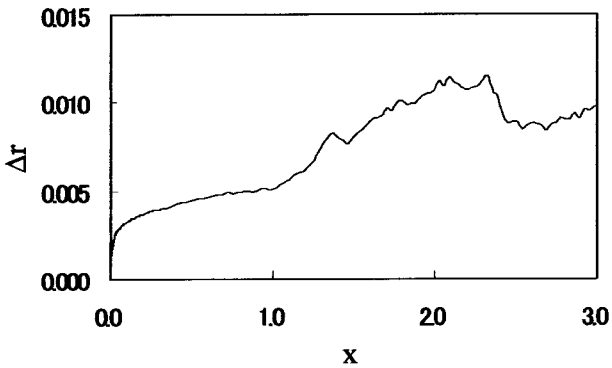

Fig. 8 Variation of thickness of reaction zone Δr with x

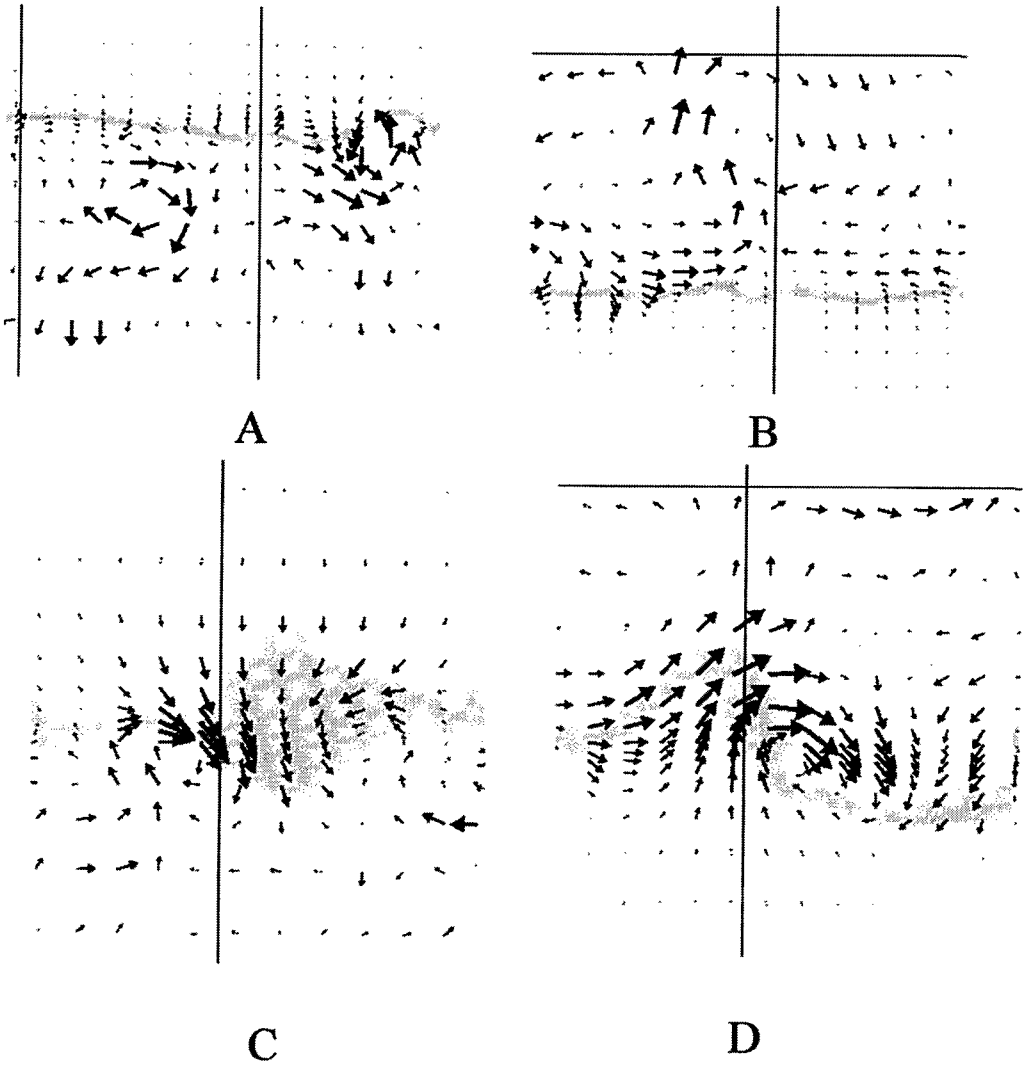

Fig. 9 Instantaneous contour of $Y_F Y_O$ and velocity vectors (v, w) on zones A, B, C and D depicted in Fig. 6.

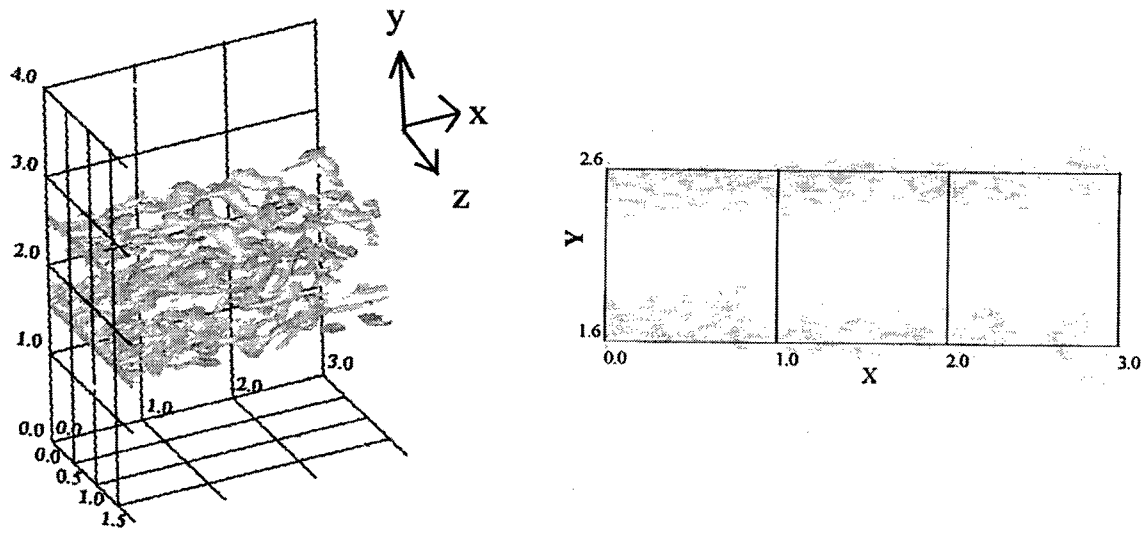

(a) three dimensional view

(b) View parrallel to z axis

Fig. 10 Turbulent vorticies visualized by second invariant of velocity gradient tensor

the wall channel flow, released to the open space holds its shape, longitudinal structure till x=1.0. They change their shape and directions at the downstream region. Some large vortices are observed in downstream region and direction of vortices change from streamwise direction (upstream) to random-like directions (downstream). Locations in y axis, 1.6 and 2.6, depicted in Fig. 10 (b) are the point where walls of channel are placed. Vortices are located inner side till x<1.0 and expand toward the outer region at the downstream. Thus, changes of turbulent vortices show a drastic change at the downstream region, x>1.0, which have a large effect on the change of the reaction zone.

CONCLUSIONS

Direct numerical simulation of spatially developing turbulent reaction jet was calculated and the reaction characteristics was analyzed. Fully developed turbulent channel flow was introduced to the inlet to form the fully developed turbulence to the inlet. Reactants F and O are in turbulent jet and in surrounding flows, respectively. Following conclusions are obtained.

(1) Increasing rate of product P increases at the region further than a distance similar to that of channel width from the inlet. It is caused by the increase of thickness of the reaction zone, not its length.

(2) Increase of reaction zone thickness is not uniform, some cloud-like regions are formed. They are formed by a change of vortical structure , direction of vortical axis and expansion of the locations toward the outer region.

The present study showed a characteristic reaction process near the outlet of fully developed wall channel flow, where reactants meet each other. Further study is now conducting at the downstream region where large vortex structure exists.

REFERENCES

Brown, G.L., Roshko, A., 1974, "On density effects and large structure in turbulent mixing layers", J. Fluid. Mech., Vol. 64, Part 4, pp 775-816

Hilbert, R., Tap, F., Veynante, D., Thevenin, D., 2002, "A New modeling approach for the autoignition of a nonpremixed turbulent flame using DNS", 29th International Symposium on combustion, pp 1-26

Li, Y., Tanahashi, M. and Miyauchi, T., 1999, "Interaction between hydrogen-air diffusion flame and large-scale vortical structure in mixing layer", Proceeding of the Second Asia-Pacific Conference on Combustion, pp. 370-373.

Mahalingam, S., Chen, JH., Vervisch, L., 1995, "Finite-rate chemistry and transient effects in direct numerical simulations of turbulent nonpremixed flames", Combust. Flame, Vol 102, No.3, pp.285-97

McMurtry, P.A., Riley, J.J., Metcalfe, R.W., 1989, "Effects of heat release on the large-scale structure in turbulent mixing layers", J. Fluid. Mech., Vol. 199, pp. 297-332

Miyauchi, T., Tanahashi, M., Suzuki, M. and Tokuda, S., 1996, "Structure analysis of spatially developing turbulent mixing layer with mixing transition", Trans. Jpn. Soc. Mech. Eng., (in Japanese), Vol. 62, No. 594, B, pp. 499-506.

Rai, M.M. and Moin, P., 1991, "Direct simulations of turbulent flow using finitedifference schemes", J. Comput. Phys., Vol. 96, pp. 15-53

Soteriou, M.C., Ghoniem, A.F., 1995, "On the application of the infinite reaction rate model in the simulation of the dynamics of exothermic mixing layers", Combust Sci. and Tech., vol. 105, pp. 377-397

Velvisch, L., Poinsot, T., 1998, "Direct numerical simulation of non-premixed turbulent flames", Annu. Rev. Fluid. Mech., Vol. 30, pp. 655-691

ACKNOWLEDGMENTS

The authors wish to express thanks to Prof. Toshio Miyauchi and Prof. Mamoru Tanahashi (Tokyo Inst. Tech.) for their assistance in using super-computer. We also thanks to Prof. Takeo Kajishima (Osaka Univ) for providing computer program of wall turbulent channel flow.